

## Force and conductance jumps in atomic-scale metallic contacts

T. N. Todorov and A. P. Sutton

*Department of Materials, University of Oxford, Parks Road, Oxford OX1 3PH, England, United Kingdom*

(Received 12 July 1996)

We have performed dynamic simulations of the pull off of a Au contact at a temperature of 1 K. The conductance and the tensile force on the contact are calculated throughout the pull off. There are prominent jumps both in the conductance and in the force. The force and conductance jumps generally coincide with each other, and correspond to abrupt atomic rearrangements in the contact. The correlation between the force and conductance jumps and the effective spring constant of the contact during pull off are in agreement with recent experiments. [S0163-1829(96)50744-7]

Several years ago, scanning tunneling<sup>1</sup> and atomic force<sup>2</sup> microscopes, and a mechanically controllable break junction<sup>3</sup> were used to generate atomic-scale metallic contacts.<sup>4,5,3</sup> These experiments raised the question of the relation between the mechanical and electrical properties of the contacts. In a typical experiment, a contact is formed between a metallic tip and substrate or between two metallic asperities, and the small-voltage dc conductance is then measured during contact pull off or compression. During these processes, the measured conductance exhibits abrupt jumps.<sup>3,6</sup>

In early molecular dynamics (MD) simulations<sup>7,8,23</sup> it was seen that the mechanical evolution of the contact proceeds through a series of abrupt atomic rearrangements in which the length and the cross-section of the contact change sharply. These rearrangements are separated by longer periods of elastic deformation, during which the overall atomic geometry of the contact remains constant. MD simulations showed that each rearrangement is reflected in an abrupt reduction in the magnitude of the force of the contact.<sup>23</sup> MD simulations and simultaneous conductance calculations<sup>9</sup> revealed that the atomic rearrangements generally result in sharp jumps in the electronic conductance of the contacts, providing an explanation for the conductance jumps seen in the experiments. However, there is an alternative explanation—conductance jumps could result from the closing off or opening up of individual conductance channels during a perfectly gradual variation in the contact cross section.<sup>10</sup> As a result, recently there has been much discussion about the occurrence of the atomic rearrangements and the correlation between them and the conductance jumps.<sup>10-14</sup>

In the past year, there have been reports of experiments in which the conductance is measured simultaneously with the force on the contact during entire excursions of contact compression and pull off.<sup>15-18</sup> A representative set of experimental results for the pull off of a Au contact at 300 K in ambient conditions is shown in Fig. 1. There are jumps both in the conductance and in the force. Furthermore, the jumps in the conductance generally coincide with those in the force. The abrupt force relaxations, in which the tensile force drops in magnitude, provide evidence for the occurrence of atomic rearrangements in the contact. The results corroborate the view that the conductance jumps generally occur in response to atomic rearrangements. The picture from Fig. 1 is consistent

with measurements under UHV conditions,<sup>17,18</sup> in which, at least for contacts with conductances less than about  $15 \times 2e^2/h$ , the magnitude of the tensile force has maxima in the vicinity of the conductance jumps.

In response to these experiments, we have performed calculations in which the force and the conductance are computed simultaneously during a dynamic simulation of the pull off of a Au contact. The conductance calculation uses explicitly the atomic coordinates from the simulation through a tight-binding model. The temperature was set to 1 K to reduce thermal fluctuations in the calculated quantities. In full agreement with the experiments, we find force and conductance jumps which coincide with each other and correspond to abrupt atomic rearrangements.<sup>9,12</sup> These findings

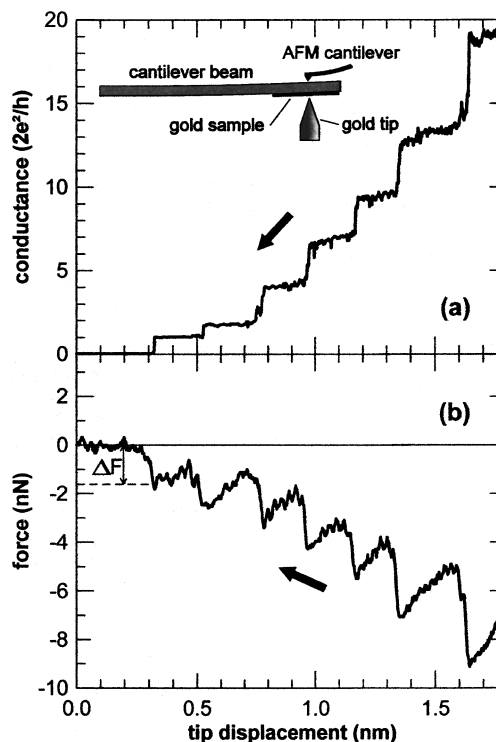


FIG. 1. The measured force and conductance during the pull off of a Au contact at 300 K. The force is measured with a cantilever beam of effective spring constant of 25 N/m. The plot is reproduced from Ref. 16 with the permission of the authors.

are consistent also with past calculations in which the conductance is computed through a free-electron jellium model assuming a rectangular contact cross section with an area and eccentricity fitted to simulation geometries.<sup>13</sup> The calculational method has been described in detail elsewhere.<sup>9,12</sup> In the dynamic simulation, an initially paraboloidal Au tip with a radius of curvature of one lattice parameter is brought into contact with a Au substrate. Once a sizeable contact area is established, the tip is pulled off the substrate, while the applied tensile force and the conductance are calculated at every step. Atomic interactions are described by the potential<sup>19</sup>

$$E = \epsilon \left\{ \frac{1}{2} \sum_i \sum_{j \neq i} \left( \frac{a}{r_{ij}} \right)^n - c \sum_i \left[ \sum_{j \neq i} \left( \frac{a}{r_{ij}} \right)^m \right]^{1/2} \right\}, \quad (1)$$

where  $r_{ij}$  is the distance between atoms  $i$  and  $j$ ,  $\epsilon = 1.2793 \times 10^{-2}$  eV,  $m = 8$ ,  $n = 10$ ,  $c = 34.408$ , and  $a = 0.408$  nm is the fcc lattice parameter. The potential is truncated at  $2.001a$ . The tip contains 287 atoms. It is attached to a rectangular slab of 1620 atoms, comprising 6 (111) planes. The tip and slab have the same crystal orientation with the [111] direction along the axis of the contact. Periodic boundary conditions are applied in the three orthogonal directions of the slab. The equations of motion of the atoms are integrated via the velocity Verlet algorithm,<sup>20</sup> and a Nosé-Hoover thermostat is applied<sup>8</sup> to all atoms in the cell. The time step in the simulations is  $10^{-14}$  s. We have performed runs with two different pull-off rates— $10^{-4}a$  per time step (4.08 m/s) and  $10^{-5}a$  per time step (0.408 m/s). The pull-off rate of  $10^{-4}a$  (or  $10^{-5}a$ ) per time step is imposed every tenth time step by applying a homogeneous tensile strain of  $10^{-3}a/L$  (or  $10^{-4}a/L$ ) normal to the slab to all atoms in the computational cell, where  $L$  is the current length of the computational cell. Each application of the strain increases the spacing between neighboring (111) atomic layers along the contact by less than 0.01% (or 0.001%). In the nine time steps before the next application of the strain atoms follow Newtonian equations of motion modified by the thermostat.

The calculation of the conductance employs an orthonormal nearest-neighbor  $1s$  tight-binding model with a half-filled band. The hopping integral  $H_{ij}$  between atoms  $i$  and  $j$  decays smoothly to zero between first- and second-nearest neighbors, and is taken as  $H_{ij} = A$  for  $z_{ij} < z_n$ , and  $2H_{ij} = A \{1 + \cos \pi[(z_{ij} - z_n)/(z_c - z_n)]\}$  for  $z_n \leq z_{ij} \leq z_c$ . Here,  $A$  is the nearest-neighbor hopping integral in the perfect fcc crystal,  $z_{ij}$  is the distance between atoms  $i$  and  $j$  in units of the ideal nearest-neighbor separation,  $z_n = (1 + \sqrt{2})/2$  and  $z_c = \sqrt{2}$ . Periodic boundary conditions are not used in the conductance calculation. Instead, the slabs above and below the tip are replaced by semi-infinite perfect crystals. We imagine that the tip atoms are initially decoupled from each other and from the substrate atoms. The tip atoms are then coupled to each other and to the substrate atoms by a coupling  $V$ , containing the respective hopping integrals. The low-voltage, low-temperature conductance  $G$  of the fully coupled system is given by<sup>21</sup>

$$G = \frac{2e^2}{h} 4\pi^2 \text{Tr}[\rho_1^0(E_F) t^\dagger(E_F) \rho_2^0(E_F) t(E_F)], \quad (2)$$

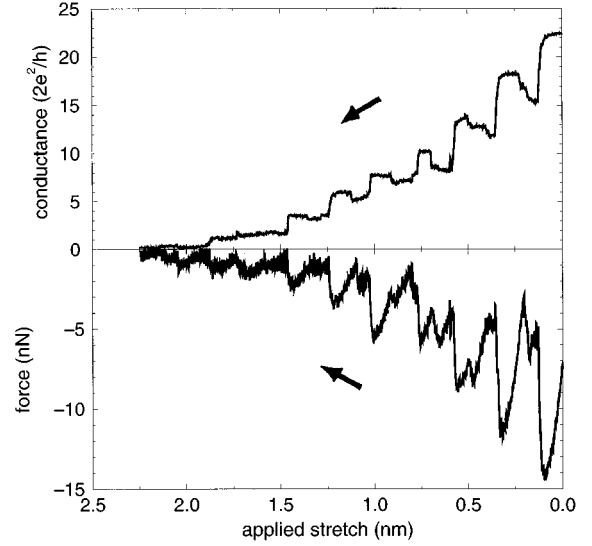


FIG. 2. The force and conductance throughout a dynamic simulation of the pull off of a Au contact at 1 K, with a pull-off rate of 4.08 m/s.

where  $t(E) = V + VG^+(E)V$ ,  $G^+(E)$  is the retarded Green function for the final coupled system,  $\rho_j^0 = [G_j^{0-}(E) - G_j^{0+}(E)]/2\pi i$  with  $j = 1, 2$  are the density of states operators for the two separate substrates, and  $E_F$  is the Fermi energy. Here,  $G_j^{0\pm}(E)$  with  $j = 1, 2$  are the retarded and advanced Green functions for the two substrates in the initial decoupled system. The conductance and the tensile force on the contact are calculated every tenth time step in the faster run and every one-hundredth time step in the slower run.

Figure 2 shows the force and the conductance during contact pull off at the higher rate of  $10^{-4}a$  per time step, or 4.08 m/s. A negative sign corresponds to a tensile force. The force goes through stages of increasing magnitude, separated by abrupt relaxations in which the magnitude of the force drops sharply. The regions of increasing force magnitude correspond to elastic elongation of the contact. The gradient of the force is approximately constant during an individual elastic stage, and decreases from one elastic stage to the next, as the contact gets thinner. Each force relaxation marks the onset of a sudden yield process, in which the contact undergoes mechanical restructuring in order to release the strain energy that has built up during the preceding elastic stage.

The conductance shows abrupt jumps separated by plateaus. Every drop in the conductance corresponds to an abrupt reduction in the tensile force. In the corresponding mechanical rearrangement, the contact elongates by one atomic layer and the contact cross-section is reduced. The plateaus correspond to the elastic elongation stages. Occasionally, particularly in the early stages of the pull off, there are regions of suppressed conductance immediately after a jump and before the following conductance plateau. These regions correspond to intermediate geometries in which the contact has some structural defect, e.g., a stacking fault, caused by the passage of a partial dislocation across the contact and producing increased electron backscattering.<sup>12</sup> Recovery from these intermediate geometries also typically occurs as an atomic rearrangement, e.g., the passage of a

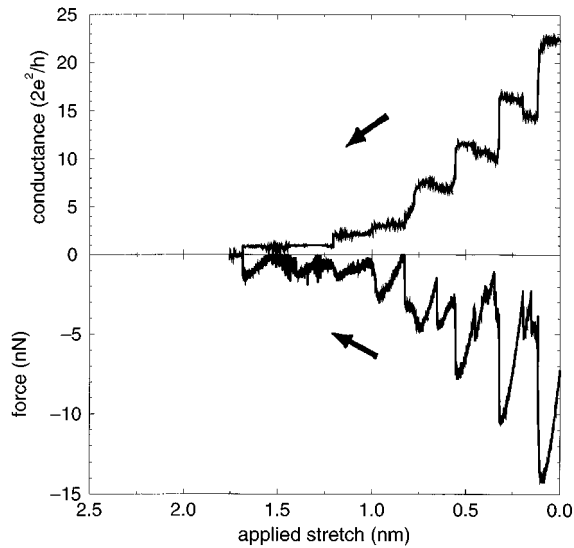


FIG. 3. The force and conductance throughout a dynamic simulation of the pull off of a Au contact at 1 K, with a pull-off rate of 0.408 m/s.

second partial dislocation across the contact eliminating the stacking fault. The recovery is reflected in a small upward conductance jump and a small force relaxation.

Figure 3 shows the force and the conductance during contact pull off at the lower rate of  $10^{-5}a$  per time step, or 0.408 m/s. This simulation involved over four hundred thousand MD time steps. The early stages of the pull off are similar to those with the higher strain rate. Larger differences develop in the later stages of the pull off, where the conductance drops to just several units of  $2e^2/h$  and the narrowest part of the contact is only several atoms across.

We suggest two reasons for these differences. At the actual atomic rearrangements the system is mechanically unstable. At those points, a small change in the atomic positions may result in an observable change in the geometry after the rearrangement is completed. The two simulations contain different numbers of time steps with differing individual geometries. By the above argument, it may be expected that the outcome of an individual rearrangement may change from one simulation to the next. Once such a difference appears, even if it involves just one atom, the two simulations stop being directly comparable to each other and, in general, they subsequently diverge further apart. Indeed, we have observed that even with the same strain rate, a difference in the initial atomic positions of less than  $10^{-4}a$  results in a visible subsequent divergence both in the absolute values of the conductance and in the positions of the conductance jumps.

The second reason for the difference between the two simulations is related to the time scales for the mechanical relaxation processes in the contacts. There is a spectrum of such processes, with time scales ranging over many orders of magnitude. The fastest relaxation mechanism consists in the response of individual atoms to the applied strain. In this process, the time scale for which is of the order of the atomic thermal vibration period, each atom continually adjusts its average position seeking to remain in a local energy minimum. Then there is a hierarchy of collective, many-atom

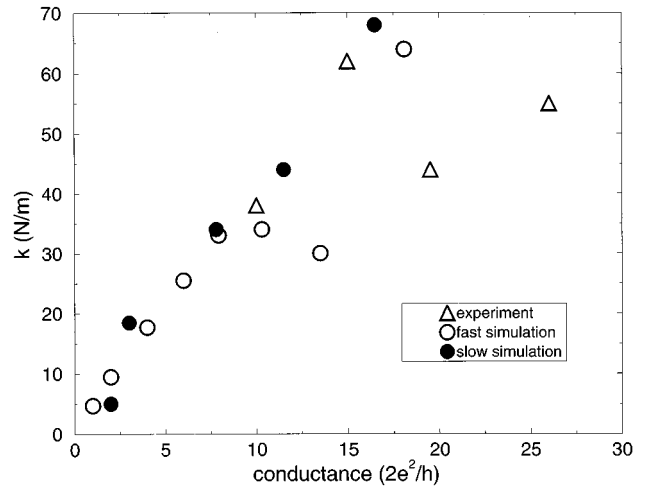


FIG. 4. The effective spring constant  $k$  of the contact plotted against the contact conductance, from both simulations and from experiment. The experimental points are taken from Ref. 16 but not from the same set of results as in Fig. 1.

relaxation mechanisms, such as strain localization in the neck and those that bring about the change of shape of the contact to minimize its total energy. As the strain rate is decreased, or the temperature raised, further and slower relaxation processes are gradually enabled, with corresponding differences in the mechanical evolution of the contact. In fact, experimentally it is found<sup>22</sup> that Au and Cu contacts with conductances less than about  $10 \times 2e^2/h$ , at room temperature, undergo fracture by themselves, without any applied stretching, over time scales of the order of seconds. This type of self-relaxation, in which the system seeks to decrease its energy by spontaneously decreasing its free surface over macroscopic time scales, shows that the contacts are intrinsically unstable in a global sense. The result of any given simulation or experiment may thus depend not only on the applied strain rate, but also on the actual total *duration* of the respective run. In the present simulations, both strain rates are much higher than in the experiments: the simulation with the lower strain rate extends over about 4 ns whereas a typical experimental scan lasts about 50 ms. In general, current MD simulations of contact fracture are limited to 10–100 ns or less, giving a difference in time scales of at least five orders of magnitude relative to a typical experiment. Nonetheless, as the strain rate in the simulation is lowered one would expect collective relaxation processes to be enhanced, particularly if they involve only a few atoms, as in the evolution of the shape of the neck in the final stages of the pull off. This would also be consistent with the divergence between the two simulations.

However, the presence of force and conductance jumps, and the correlation between them, can be seen clearly in the results of both simulations. The slope of the force versus stretch curves in the elastic stages can be used to estimate an effective spring constant  $k$  for the contact. Figure 4 shows the estimated  $k$  versus the conductance of the contact for the two simulations together with experimental points from reference<sup>16</sup> (not from the same set of results as in Fig. 1). The details of the three sets of results are different. This may

be expected since  $k$  depends not only on the radius of the constriction, but also on the overall shape of the contact<sup>16</sup> and the latter cannot be expected to reproduce in detail. However, the overall agreement between the three sets of results is good. The rough magnitude of  $k$  is the same in each case. Both the calculated and the experimental results show oscillations in the  $k$  versus conductance curves.

Finally, both experiments and calculations show some conductance plateaus, particularly in the final stages of the pull off, that are quantized in units of  $2e^2/h$ , and others that are not. For example, the last two plateaus in Fig. 3 are very close to 2 and 1 quantum units, respectively, while earlier plateaus are sloped and noisy. At the same time, in each case the transitions between neighboring plateaus are accompanied by force jumps, indicating underlying atomic rearrangements. These observations show that there is no contradiction between individual conductance plateaus being quantized, and the respective contact geometries being linked by abrupt rearrangements.<sup>12,13</sup>

In conclusion, we have calculated the conductance and the tensile force throughout dynamic simulations of the pull off of a Au contact at 1 K with strain rates of 4.08 m/s and 0.408 m/s. The details of the two simulations are different, the differences being more prominent in the later stages of the pull off. These differences reflect the presence of a hierarchy of relaxation mechanisms, with different characteristic time scales. Qualitatively, with both pull-off rates, the contact evolves through a series of mechanical rearrangements. Each rearrangement is reflected in an abrupt reduction in the force and a corresponding conductance jump. The correlation between the force and conductance jumps, the size of the forces and the effective spring constant of the contact during the pull off agree with experiment.

The authors are grateful to G. Rubio, N. Agrait and S. Vieira for the permission to reproduce the experimental plot shown in Fig. 1 and for suggesting Fig. 4. We thank J. B. Pethica for many discussions. The calculations were carried out in the Materials Modelling Laboratory. TNT is grateful to St. John's College, Oxford, for financial support.

- 
- <sup>1</sup>G. Binnig, H. Rohrer, Ch. Gerber, and E. Weibull, *Phys. Rev. Lett.* **49**, 57 (1982).
- <sup>2</sup>G. Binnig, C. F. Quate, and Ch. Gerber, *Phys. Rev. Lett.* **56**, 930 (1986).
- <sup>3</sup>C. J. Muller, J. M. van Ruitenbeek, and L. J. de Jongh, *Phys. Rev. Lett.* **69**, 140 (1992).
- <sup>4</sup>J. K. Gimzewski and R. Möller, *Phys. Rev. B* **36**, 1284 (1987).
- <sup>5</sup>U. Dürig, O. Züger, and D. W. Pohl, *Phys. Rev. Lett.* **65**, 349 (1990).
- <sup>6</sup>J. M. Krans, C. J. Muller, I. K. Yanson, Th. C. M. Govaert, R. Hesper, and J. M. van Ruitenbeek, *Phys. Rev. B* **48**, 14 721 (1993).
- <sup>7</sup>A. P. Sutton and J. B. Pethica, *J. Phys. Condens. Matter.* **2**, 5317 (1990).
- <sup>8</sup>A. P. Sutton, J. B. Pethica, H. Rafii-Tabar, and J. A. Nieminen, in *Electron Theory for Alloy Design*, edited by D. G. Pettifor and A. H. Cottrell (Institute of Materials, London, 1992), Chap. 7.
- <sup>9</sup>T. N. Todorov and A. P. Sutton, *Phys. Rev. Lett.* **70**, 2138 (1993).
- <sup>10</sup>L. Olesen, E. Laegsgaard, I. Stensgaard, F. Besenbacher, J. Schiøtz, P. Stolze, K. W. Jacobsen, and J. K. Nørskov, *Phys. Rev. Lett.* **72**, 2251 (1994).
- <sup>11</sup>J. M. Krans, C. J. Muller, N. van der Post, F. R. Postma, A. P. Sutton, T. N. Todorov, and J. M. van Ruitenbeek, *Phys. Rev. Lett.* **74**, 2146 (1995).
- <sup>12</sup>A. M. Bratkovsky, A. P. Sutton, and T. N. Todorov, *Phys. Rev. B* **52**, 5036 (1995).
- <sup>13</sup>M. Brandbyge, J. Schiøtz, M. R. Sorensen, P. Stoltze, K. W. Jacobsen, J. K. Nørskov, L. Olesen, E. Laegsgaard, I. Stensgaard, and F. Besenbacher, *Phys. Rev. B* **52**, 8499 (1995).
- <sup>14</sup>J. A. Torres and J. J. Saenz, *Physica B* **218**, 234 (1996).
- <sup>15</sup>N. Agrait, G. Rubio, and S. Vieira, *Phys. Rev. Lett.* **74**, 3995 (1995).
- <sup>16</sup>G. Rubio, N. Agrait, and S. Vieira, *Phys. Rev. Lett.* **76**, 2302 (1996).
- <sup>17</sup>A. Stalder and U. Dürig, *Appl. Phys. Lett.* **68**, 637 (1996).
- <sup>18</sup>A. Stalder and U. Dürig, *J. Vac. Sci. Technol. B* **14**(2), 1259 (1996).
- <sup>19</sup>A. P. Sutton and J. Chen, *Philos. Mag. Lett.* **61**, 139 (1990).
- <sup>20</sup>M. P. Allen and D. J. Tildesley, *Computer Simulation of Liquids* (Oxford University Press, Oxford, 1987).
- <sup>21</sup>T. N. Todorov, G. A. D. Briggs, and A. P. Sutton, *J. Phys. Condens. Matter.* **5**, 2389 (1993).
- <sup>22</sup>C. J. Muller, J. M. Krans, T. N. Todorov, and M. A. Reed, *Phys. Rev. B* **53**, 1022 (1996).
- <sup>23</sup>U. Landman, W. D. Luedtke, N. A. Burnham, and R. J. Colton, *Science* **248**, 454 (1990).